Impact of LHC top-quark pair measurements to CTEQ-TEA PDF analysis

Orkash Amat

School of Physics Science and Technology, Xinjiang University, Urumqi, Xinjiang 830046 China
E-mail:`orkaxmamat@163.com`

Michał Czakon

Institut für Theoretische Teilchenphysik und Kosmologie, RWTH Aachen University, D-52056
Aachen, Germany
E-mail:`mczakon@physik.rwth-aachen.de`

Sayipjamal Dulat

School of Physics Science and Technology & Center for Theoretical Physics,
Xinjiang University, Urumqi, Xinjiang 830046 China
E-mail: `sdulat@hotmail.com`

Tie-Jiun Hou[*]

Department of Physics, College of Sciences, Northeastern University, Shenyang 110819, China
E-mail: `houtiejiun@mail.neu.edu.cn`

Joey Huston

Department of Physics and Astronomy, Michigan State University, East Lansing, MI 48824
U.S.A.
E-mail: `Huston@pa.msu.edu`

Alexander Mitov

Cavendish Laboratory, University of Cambridge, Cambridge CB3 0HE, UK
E-mail:`adm74@cam.ac.uk`

Andrew S. Papanastasiou

Cavendish Laboratory, University of Cambridge, Cambridge CB3 0HE, UK
MRC Institute of Genetics and Molecular Medicine, University of Edinburgh, Crewe Road,
Edinburgh EH4 2XU, UK
E-mail:`apapanas@inf.ed.ac.uk`

Carl Schmidt

Department of Physics and Astronomy, Michigan State University, East Lansing, MI 48824
U.S.A.
E-mail: `schmidt@pa.msu.edu`

Ibrahim Sitiwaldi

School of Physics Science and Technology & Center for Theoretical Physics,
Xinjiang University, Urumqi, Xinjiang 830046 China
E-mail: `ibrahim010@sina.com`

Keping Xie

Department of Physics, Southern Methodist University, Dallas, TX 75275-0181, U.S.A.
E-mail: `kepingx@mail.smu.edu`

Zhite Yu
Department of Physics and Astronomy, Michigan State University, East Lansing, MI 48824
U.S.A.
E-mail: `yuzhite@msu.edu`

C.-P. Yuan
Department of Physics and Astronomy, Michigan State University, East Lansing, MI 48824
U.S.A.
E-mail: `yuan@pa.msu.edu`

Detailed studies have been carried out on the impact of the LHC top quark pair production data on gluon PDF, in the context of the CTEQ-TEA global PDF fit, with the ePump-updating method. The considered $t\bar{t}$ data include single differential distributions from ATLAS and double differential distributions from CMS, both at 8 TeV. All analyses have been carried out at the NNLO, using fastNNLO tables. We show that the sensitivity per data point of the LHC $t\bar{t}$ data is similar to that of jet data, as included in the CT14HERA2 fit, while the total sensitivity of the present $t\bar{t}$ data is not as large as the jet data because of the much smaller number of $t\bar{t}$ data points in the presently available data.

---

*Speaker.

The top-quark pair production is a brand new observable available for global analysis in CTEQ-TEA PDFs after CT14HERA2 [1]. For experimental side, we consider the absolute and normalized one-dimensional p_T, y_t, $m_{t\bar{t}}$ and $y_{t\bar{t}}$ distributions from ALTAS [3] and CMS [4], and the two-dimensional distributions from CMS [5]. Theory prediction is done at the NNLO QCD with $\mu_R, \mu_f = \frac{H_T}{4}$ or $\frac{m_T}{4}$ through fastNLO grids [7, 8]. Instead of implementing in real global analysis, we study the impact of top-quark pair production on PDFs in the framework of CT14HERA2 by using ePump (Error PDF Updating Method Package) [6].

Observable	Detector		Npts	χ^2/N
inclusive jet	CDF	[10]	72	1.50
inclusive jet	D0	[11]	110	1.03
inclusive jet	ATLAS	[12]	90	0.57
inclusive jet	CMS	[13]	133	0.93
$\frac{1}{\sigma}\frac{d\sigma}{dp_T^t}$	ATLAS, CMS	[3, 4]	8,8	0.39, 3.88
$\frac{1}{\sigma}\frac{d\sigma}{dy_t}$	ATLAS, CMS	[3, 4]	5,10	2.70, 2.53
$\frac{1}{\sigma}\frac{d\sigma}{dm_{t\bar{t}}}$	ATLAS, CMS	[3, 4]	7,7	0.25, 8.67
$\frac{1}{\sigma}\frac{d\sigma}{dy_{t\bar{t}}}$	ATLAS, CMS	[3, 4]	5,10	2.46, 3.67
$\frac{d\sigma}{dp_T^t}$	ATLAS	[3]	8	0.34
$\frac{d\sigma}{dy_t}$	ATLAS	[3]	5	3.18
$\frac{d\sigma}{dm_{t\bar{t}}}$	ATLAS	[3]	7	0.45
$\frac{d\sigma}{dy_{t\bar{t}}}$	ATLAS	[3]	5	4.65
$d^2\sigma/dy_t dp_T^t$	CMS	[5]	16	1.23
$d^2\sigma/dm_{t\bar{t}} dp_T^{t\bar{t}}$	CMS	[5]	16	2.01
$d^2\sigma/dm_{t\bar{t}} d\Delta\eta_{t\bar{t}}$	CMS	[5]	12	1.70
$d^2\sigma/dm_{t\bar{t}} dy_t$	CMS	[5]	16	1.28
$d^2\sigma/dm_{t\bar{t}} dy_{t\bar{t}}$	CMS	[5]	16	1.27

Table 1: Number of data points and χ^2/Npts for incl. jet and top-quark pair data, after ePump updating from the CT14HERA2mjet PDFs.

With direct implementation of ePump updating, we see no significant impact from the 1D $t\bar{t}$ distributions on modifying the CT14HERA2 PDFs except some minor change on gluon PDF in the large-x region. This simply means that the gluon PDF, in the x range relevant to the 1D $t\bar{t}$ distributions, is already constrained by some other data in the original CT14HERA2 fit. As shown in Ref.[9], in the framework of CT14HERA2, the gluon PDFs are mainly constrained by DIS and jet data. In order to see the impact on gluon PDF from $t\bar{t}$ production, we need to suppress the contribution from jet data. For this purpose, the Hessian eigenvector sets CT14HERA2mjet are generated from a global fit by including all the data used in the CT14HERA2 fit except the four inclusive jet production data from the Tevatron and the LHC Run I.

Without the jet data included in the starting CT14HERA2mjet PDFs, the ePump updated PDFs that include only the $t\bar{t}$ data in the analysis, receive no contribution from jet data. In Fig. 1, we show both ePump updated PDFs, starting from CT14HERA2 and CT14HERA2mjet PDFs by including

the normalized ATLAS 8 TeV $y_{t\bar{t}}$ data. The impact on gluon PDF from $t\bar{t}$ data can be seen by comparing the difference between the gluon PDF before and after the ePump updating. We note that, we do not include the PDF errors induced by the two extreme g-PDF sets of CT14HERA2 PDFs in this work, for fair comparison of various PDF error sets. It is obvious that, without the jet data included in the global analysis, the normalized $t\bar{t}$ data have rather obvious impact on both the central predictions and uncertainty bands of the CT14HERA2mjet PDFs. Hence, the $t\bar{t}$ data can indeed constrain the g-PDF in the large-x region.

The ePump-updated CT14HERA2mjet gluon-PDFs after adding all those four jet data (named CT14HERA2mjetpjet) and adding only CMS 7 TeV jet data (named CT14HERA2mjetpCMS7jet) are also compared in Fig. 1. We first observe that, the CT14HERA2mjetpjet gluon PDF has much smaller uncertainty band than the CT14HERA2mjetpATLAS8Nytt gluon PDF for x between 0.01 and 0.3, which shows the much stronger constrain on the gluon PDF uncertainty from the jet data. It is therefore understandable why we did not see significant impact on the ePump-updated CT14HERA2 PDF by including the $t\bar{t}$ data. Despite the noticeable difference between the uncertainty bands of CT14HERA2mjetpjet and CT14HERA2mjetpATLAS8Nytt gluon PDFs, it is worth noting that both the $t\bar{t}$ and jet data constrain the central-fit g-PDF in a similar way. They all prefer softer gluon in the large-x region, as compared to the CT14HERA2mjet fit.
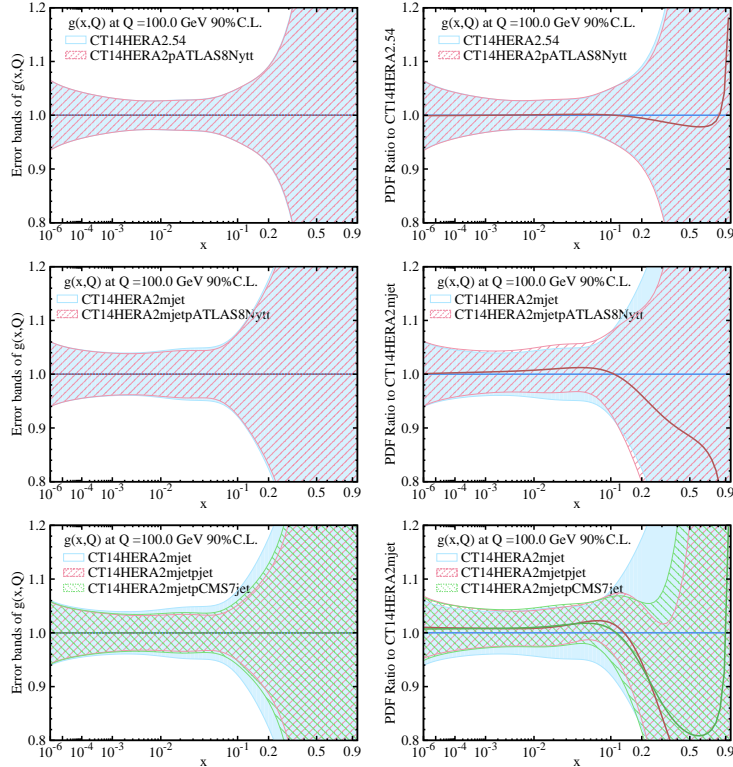

Figure 1: ePump updated PDFs, CT14HERA2pATLAS8Nytt and CT14HERA2mjetpATLAS8Nytt, which are obtained by including normalized ATLAS 8 TeV $y_{t\bar{t}}$ data, are compared with the PDFs before the updating, which are CT14HERA2 and CT14HERA2mjet PDFs, respectively. The CT14HERA2mjetpCMS7jet PDFs are ePump-updated from CT14HERA2mjet by adding only the CMS 7 TeV jet data.

Fig. 1 also shows that the CMS 7 TeV inclusive jet data provide the strongest constraint on the *g*-PDF among the four jet data included in the CT14HERA2 fit.

Below, we explain why the *g*-PDF error band of CT14HERA2mjetpATLAS8Nytt is not as narrow as that of CT14HERA2mjetpCMS7jet in the large-*x* region. Namely, we would explain why jet data provide stronger constraint on *g*-PDF uncertainties than the considered $t\bar{t}$ data.

First, we note that the $t\bar{t}$ data have rather smaller number of data points than the jet data, by about a factor of 10. In Table 1, we show the number of data points (*N*) for jet data that are included in the CT14HERA2 fit and for the new LHC $t\bar{t}$ data. The values of χ^2/N in the Table 1 are calculated by using ePump to update the CT14HERA2mjet PDFs with the inclusion of each individual data set. As discussed above, the sensitivity of the $t\bar{t}$ data to *g*-PDF is not as large as the jet data, to constrain the *g*-PDF uncertainties in the large-*x* region. Nevertheless, it is also interesting to compare the sensitivity per data point of the jet and $t\bar{t}$ data. In order to see this, a hypothetical weight is assigned to the 1D $t\bar{t}$ distribution data with the weight equal to the ratio between the number of data points of the CMS 7 TeV jet data and the considered $t\bar{t}$ distribution. Taking the normalized CMS 8TeV p_T distribution as an example, the hypothetical weight that applies to the data is equal to $w = 133/8 = 16.6$. In practice, a larger weight can arise from increasing the event statistics (e.g., with a larger integrated collider luminosity) or reducing the experimental errors (e.g., with improvement in detection efficiency).
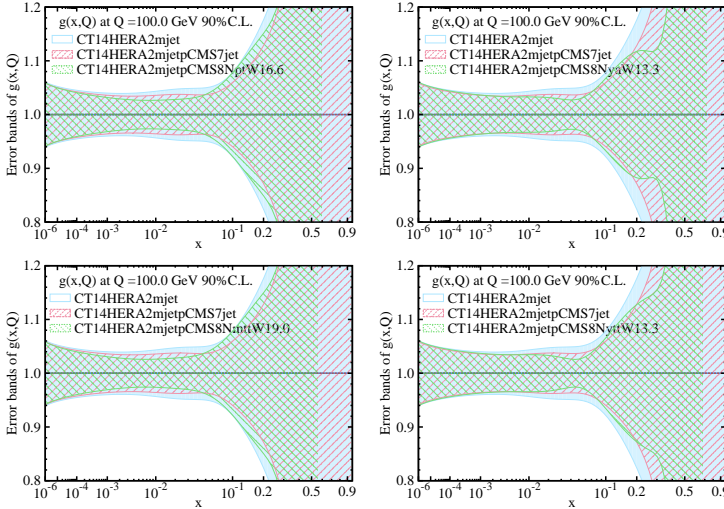

In this naive estimation, we assume the central values of the measurement do not change so that we only show the comparison on the PDF uncertainties in the following figures.

In Fig. 2, we compare the impact on *g*-PDF uncertainty from the CMS 7 TeV jet data and the normalized CMS 8TeV 1D $t\bar{t}$ distribution data, with the hypothetical weight discussed above. It shows that, the weighted $t\bar{t}$ distribution data provide stronger constraint on gluon PDFs for $10^{-3} \lesssim x \lesssim 5 \times 10^{-2}$. This conclusion also holds for the absolute ATLAS 8 TeV 1D $t\bar{t}$ distribution data. With the hy-

Figure 2: Comparison of CT14HERA2mjet and ePump-updated PDFs, at Q = 100 GeV and at 90% C.L., by adding only the CMS 7 TeV jet data or the normalized CMS 8 TeV 1D $t\bar{t}$ data, by adding one at a time, with hypothetical weights for various $t\bar{t}$ distributions.

pothetical weight equal to the ratio of the number of jet and $t\bar{t}$ data points, the absolute 1D $t\bar{t}$ distribution data provide about the same constraint on gluon PDF as the jet data, which is shown in Fig. 3.

Further examination on the absolute CMS 8 TeV two-dimentional $t\bar{t}$ distribution data also

shows no significant impact on ePump-updating CT14HERA2 and CT14HERA2mjet PDFs. Simi-
lar to the 1D $t\bar{t}$ data, the 2D $t\bar{t}$ data also show compatible sensitivity to updating the CT14HERA2mjet
gluon PDF as the jet data, when a hypothetical weight is assigned to equal to the ratio of the num-
ber of jet and $t\bar{t}$ data points, for the considered distribution. The result of comparison is shown in
Fig. 4.

Next, we examine the impact of the updated PDFs, obtained by including various $t\bar{t}$ data in the
ePump updating. The Higgs production rate through gluon-gluon fusion at the LHC is sensitive to
g-PDF in the middle-x region, which is constrained by both the jet and $t\bar{t}$ data. In Fig. 5, we show
the correlation ellipses of the Higgs production rate via gluon-gluon fusion and the CMS 8 TeV
normalized $y_{t\bar{t}}$ differential cross section (with weight 1 or 13.3, respectively), for various ePump
updating scenarios.

In summary, we ob-
serve that the present top-
quark pair production data
show minor impact on updat-
ing the CT14HERA2 gluon
PDF where some Tevatron
and LHC jet data have already
been included in the global
analysis. This is because the
number of data points for the
$t\bar{t}$ data is much less than the
jet data. Though the over-
all sensitivity of the present
$t\bar{t}$ data is smaller than the jet
data, the $t\bar{t}$ data constrain the
central-fit g-PDF in the same
way as the CMS 7 TeV jet
data. Hence, with increasing
number of $t\bar{t}$ data collected
at the future LHC runs, the
$t\bar{t}$ data can provide as strong

Figure 3: Comparison of CT14HERA2mjet and ePump-updated
PDFs, at Q = 100 GeV and at 90% C.L., by adding the CMS 7 TeV jet
data and the absolute CMS 8 TeV 1D $t\bar{t}$ data, by adding one at a time,
with hypothetical weight for various $t\bar{t}$ distributions.

constrain on g-PDF uncertainty as jet data in their common x values. It may even provide stronger
constraint than jet data in somewhat larger x values where the theoretical uncertainty of the NNLO
$t\bar{t}$ calculation can be smaller than that of the NNLO inclusive jet cross section calculation. We also
showed that the sensitivity per data point of the jet and $t\bar{t}$ data, for constraining the g-PDF in the
similar x range, are about the same. This is done by assigning a hypothetical weight to the $t\bar{t}$ data,
as the ratio of the number of total data points between jet data and the $t\bar{t}$ data under consideration.
We find that the weighted $t\bar{t}$ data can constrain g-PDF uncertainty as well as the jet data. Hence,
we conclude that the sensitivity per data point of the LHC $t\bar{t}$ data is similar to that of jet data, as
included in the CT14HERA2 fit, while the total sensitivity of the present $t\bar{t}$ data is not as large as
the jet data. This is because the sensitivity of the whole data set depends on the total number of
data points, and the total number of data points of the presently available $t\bar{t}$ data is smaller than that
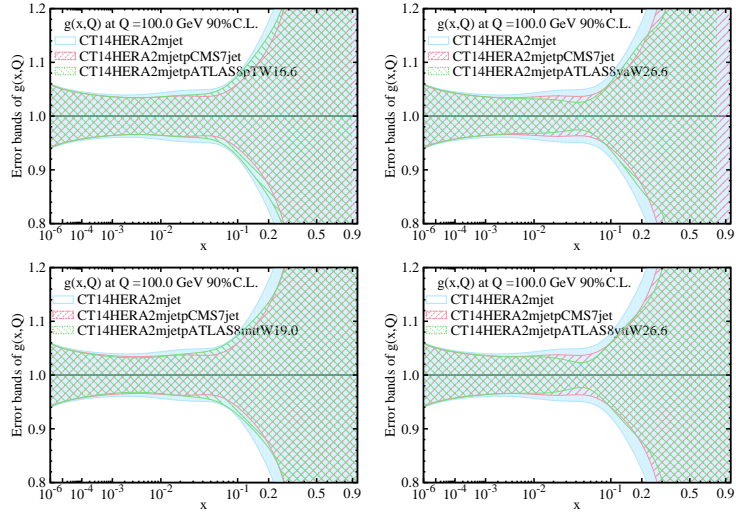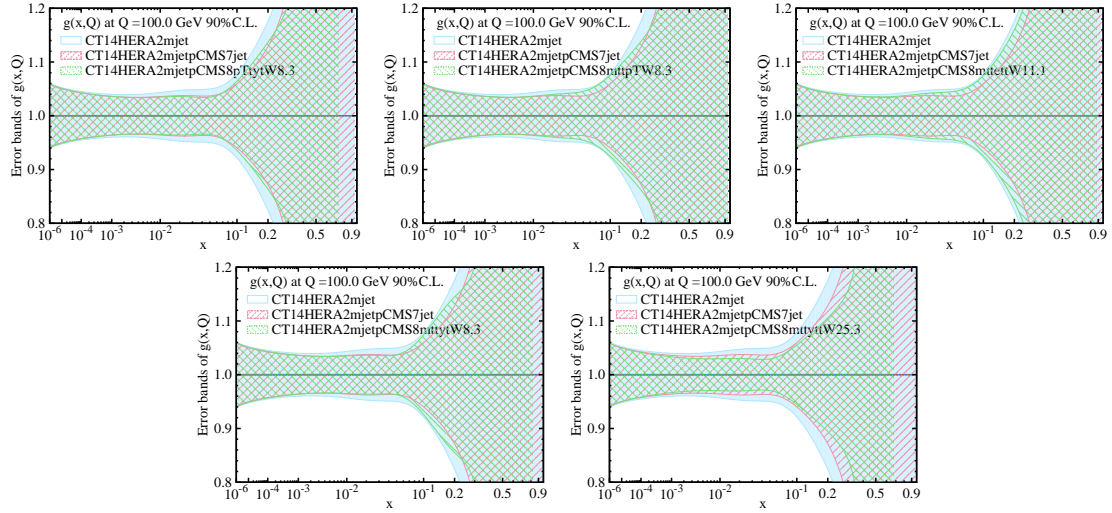
of the LHC jet data.

Figure 4: Comparison of the impact on gluon uncertainty between CMS 7 TeV jet data and the absolute CMS 8TeV 2D *tt̄* data with a hypothetical weight which equals to the ratio of the number of jet and *tt̄* data points, for the considered distribution.

Acknowledgments

References

[1] T. J. Hou *et al.*, Phys. Rev. D **95**, no. 3, 034003 (2017) doi:10.1103/PhysRevD.95.034003 [arXiv:1609.07968 [hep-ph]].

[2] G. Aad *et al.* [ATLAS Collaboration], JHEP **1502**, 153 (2015) Erratum: [JHEP **1509**, 141 (2015)] doi:10.1007/JHEP02(2015)153, 10.1007/JHEP09(2015)141 [arXiv:1410.8857 [hep-ex]].

[3] G. Aad *et al.* [ATLAS Collaboration], Eur. Phys. J. C **76**, no. 10, 538 (2016) doi:10.1140/epjc/s10052-016-4366-4 [arXiv:1511.04716 [hep-ex]].
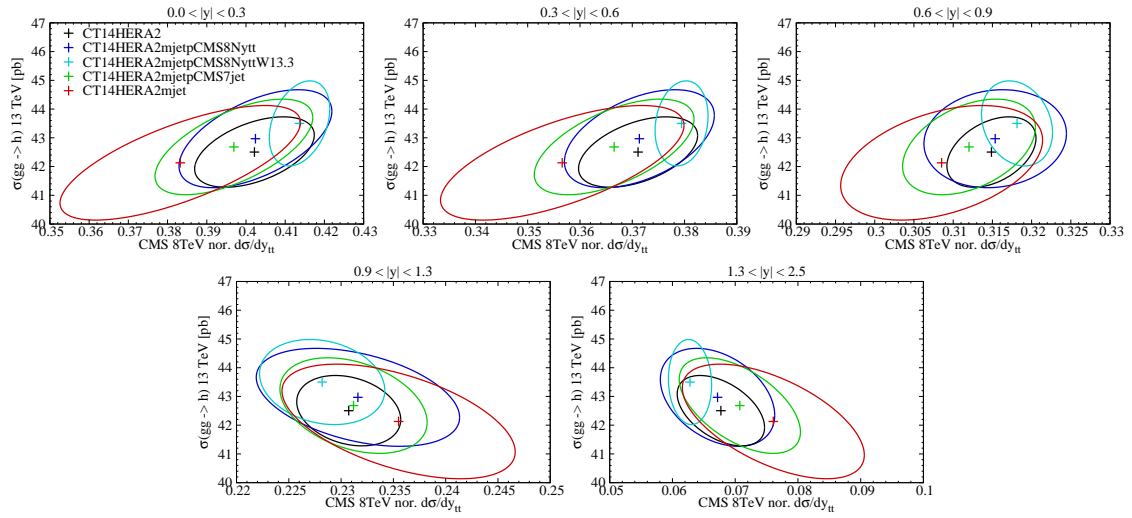
Figure 5: Correlation ellipse between CMS 8 TeV normalized $y_{t\bar{t}}$ data for various rapidity bins and Higgs production through gluon-gluon fusion at the 13 TeV LHC for CT14HERA2 (black), CT14HERA2mjetpCMS8Nytt (blue), CT14HERA2mjetpCMS8NyttW13.3 (cyan), CT14HERA2mjetpCMS7jet (green) and CT14HERA2mjet (red). The central prediction of the CT14HERA2mjetpCMS8NyttW13.3 is obtained by assuming the central measurement is the same as that in CT14HERA2mjetpCMS8Nytt.

[4] V. Khachatryan *et al.* [CMS Collaboration], Eur. Phys. J. C **75**, no. 11, 542 (2015) doi:10.1140/epjc/s10052-015-3709-x [arXiv:1505.04480 [hep-ex]].

[5] A. M. Sirunyan *et al.* [CMS Collaboration], Eur. Phys. J. C **77**, no. 7, 459 (2017) doi:10.1140/epjc/s10052-017-4984-5 [arXiv:1703.01630 [hep-ex]].

[6] C. Schmidt, J. Pumplin, C. P. Yuan, Phys. Rev. D **98**, no. 9, 094005 (2018) doi:10.1103/PhysRevD.98.094005 [arXiv:1806.07950 [hep-ph]].

[7] M. Czakon, D. Heymes and A. Mitov, JHEP **1704**, 071 (2017) doi:10.1007/JHEP04(2017)071 [arXiv:1606.03350 [hep-ph]].

[8] M. Czakon, D. Heymes and A. Mitov, fastNLO tables for NNLO top-quark pair differential distributions, arXiv:1704.08551.

[9] T. J. Hou, Z. Yu, S. Dulat, C. Schmidt and C.-P. Yuan, arXiv:1907.12177 [hep-ph].

[10] T. Aaltonen *et al.* [CDF Collaboration], Phys. Rev. D **78**, 052006 (2008) Erratum: [Phys. Rev. D **79**, 119902 (2009)] doi:10.1103/PhysRevD.79.119902, 10.1103/PhysRevD.78.052006 [arXiv:0807.2204 [hep-ex]].

[11] V. M. Abazov *et al.* [D0 Collaboration], Phys. Rev. Lett. **101**, 062001 (2008) doi:10.1103/PhysRevLett.101.062001 [arXiv:0802.2400 [hep-ex]].

[12] G. Aad *et al.* [ATLAS Collaboration], Phys. Rev. D **86**, 014022 (2012) doi:10.1103/PhysRevD.86.014022 [arXiv:1112.6297 [hep-ex]].

[13] S. Chatrchyan *et al.* [CMS Collaboration], Phys. Rev. D **87**, no. 11, 112002 (2013) Erratum: [Phys. Rev. D **87**, no. 11, 119902 (2013)] doi:10.1103/PhysRevD.87.112002, 10.1103/PhysRevD.87.119902 [arXiv:1212.6660 [hep-ex]].